



Contents lists available at ScienceDirect

## Information Sciences

journal homepage: [www.elsevier.com/locate/ins](http://www.elsevier.com/locate/ins)

# Memory-event-trigger-based secure control of cloud-aided active suspension systems against deception attacks



Xiang Sun<sup>a</sup>, Zhou Gu<sup>a,b,\*</sup>, Fan Yang<sup>a</sup>, Shen Yan<sup>a</sup>

<sup>a</sup> College of Mechanical & Electronic Engineering, Nanjing Forestry University, Nanjing, 210037, China

<sup>b</sup> Key Laboratory of Information Perception and Cooperative Control of Multi-mobiles, Nanjing, 210094, China

## ARTICLE INFO

### Article history:

Received 26 April 2020

Received in revised form 21 June 2020

Accepted 27 June 2020

Available online 19 July 2020

### Keywords:

Cloud-aided active suspension systems

Takagi-Sugeno fuzzy model

Memory-based event-triggered mechanism

Deception attacks

## ABSTRACT

This paper investigates the problem of memory-based event-triggered fuzzy control for cloud-aided active suspension systems (ASSs) against deception attacks. A novel memory-based event-triggered mechanism (ETM) which is sensitive to deception attacks is proposed. Compared to the general ETM, the system under the memory-based ETM has a higher average data releasing rate during deception attacks and external disturbance. Therefore, a better suspension performance of the cloud-aided ASS can be obtained. Meanwhile, the system without deception attacks can maintain a lower average data releasing rate, thereby reducing the occupation of the network resource. Moreover, such a memory-based ETM can mitigate the occurrence of wrong triggering event that is generated by some abrupt variation of the input of ETM. Sufficient conditions that guarantee the desired performance of cloud-aided ASSs are derived. Finally, an example of quarter-vehicle suspension system is provided to verify the effectiveness of the proposed method.

© 2020 Elsevier Inc. All rights reserved.

## 1. Introduction

In the past decades, a lot of efforts have been made to the cloud-aided vehicle suspension systems [32]. Under the framework of cloud-aided ASSs, abundant computation and data storage resources can be taken from the cloud to facilitate the implementation of predictive, optimal, and cooperative driving strategies. Compared to traditional vehicle suspension systems, a cloud-aided vehicle suspension system is much more cost-effective since it requires less quantities of complicated electronic devices for each vehicle. Moreover, cloud underpins a vast number of services including various high-performance cloud applications, therefore, the users can save a large amount of development cost. Cloud-aided ASSs signal transmission is via wireless network which may induce many new problems in control design, such as, the issues of limited bandwidth [24,30,35], cyber-attacks [13,5,2,7,1,36], etc. Meanwhile, the suspension performance, such as, ride comfort, road holding and suspension deflection are still needed to be taken into account in the design of traditional ASSs. It is noted that these network-induced problems may lead to a worse suspension performance for cloud-aided ASSs when using the traditional control design methods. Extensive research has been conducted on these meaningful and challenging issues, for example, [22,23,37], and the references therein.

The transmission protocol with periodic sampling and releasing is commonly utilized for the control of cloud-aided ASSs. The sampled-data  $H_\infty$  control was studied for ASSs in [6,10]. This transmission protocol is often called time-triggered

\* Corresponding author.

E-mail address: [gzh1808@163.com](mailto:gzh1808@163.com) (Z. Gu).

mechanism (TTM). The worst situation should be taken into account in setting the sampling and releasing period. Under this scenario, many sampling, releasing and computation are unnecessary for control systems. The ETM has been widely investigated in the past decades, by which data packets are released only when the triggering event occurs [15,14]. The average data releasing period can be largely extended under the ETM. Therefore, the limited network bandwidth can be mitigated for the networked control systems (NCSs) by using ETM [28,29,33]. In [32], the authors investigated distributed  $H_\infty$  filtering for a semi-vehicle ASS based on the ETM. To make the data releasing rate more suitable for control system, it is expected to design a reasonable ETM from the following two ways: the one is threshold, the other is triggering function. It is known that the threshold of the ETM plays a crucial role in the data releasing rate, which may further affect the control performance. The threshold is generally set by a predetermined constant, for example, in [28,31,4,19]. The authors proposed adaptive ETMs in [9,12]. Threshold of this kind of ETM dynamically varies with the state of the system.

Notice that most of the existing results regarding the ETM design use the current sampling data and the latest releasing data as the input of the ETM. In fact, the historical information is more helpful to improve the overall performance of the control system. However, few results with respect to the ETM use historical data to decide the next releasing instant for the T-S fuzzy based suspension systems, which motivates the current study.

The signal of cloud-aided ASSs is transmitted via the cloud, which is vulnerable to attacks launched by adversaries [27]. The main purpose of malicious attacks on the control system is to deteriorate or even destroy control systems besides stealing information of the system. Among attack modes, deception attack is one of the most common modes [20,25,3]. Under this type of attack, adversaries inject the false data into the transmission data. In view of the limitation of attack energy and avoidance of detection, the attack signal is usually bounded or does not deviate much from the transmitted information. Moreover, the attack is launched randomly. Nevertheless, it may lead to deterioration of suspension performance. Therefore, it is extremely essential to investigate cloud-aided ASSs subject to deception attacks. In order to get a desired suspension performance when cloud-aided ASSs suffer from deception attacks, more data packets are needed to adapt this situation, which requires the ETM to generate more triggering events during deception attacks. However, few literature focuses on this issue, which is another motivation of this study.

Motivated by the above discussion, this paper is concerned with fuzzy  $H_\infty$  control for cloud-aided uncertain ASSs against deception attacks. Taking the uncertainty of sprung mass into account, the ASS is modeled as a T-S fuzzy model. Based on this T-S fuzzy model, the memory-based fuzzy control strategy together with the memory-based ETM is proposed to ensure the suspension performance for cloud-aided ASSs subject to deception attacks. One of the main contributions of this paper is to propose a novel memory-based ETM from the following two aspects: 1) The past releasing information is introduced as the ETM input, by which wrong triggering events can be reduced since the error item in the new memory-based ETM uses the average information; 2) The improved triggering function is more sensitive to deception attacks, that is, the average data releasing rate during deception attacks is higher than other periods. Much more control information can be achieved so as to get a better suspension performance. Another main contribution is to construct a novel memory-based fuzzy control strategy, under which the suspension performance of cloud-aided ASSs can be further improved, especially for the settle time of main ASSs indicators.

The rest of this paper is summarized below. The system description and problem formulation are given in Section 2. Section 3 provides the control design of cloud-aided ASSs subject to deception attacks based on the model in Section 2. Section 4 demonstrates the design results by a simulation example. Section 5 summarizes the paper.

## 2. Problem Formulation

### 2.1. System description and performance indicators

A quarter-vehicle ASS is shown in Fig. 1. The kinetic equations of the system can be expressed by the following model [10]

$$\begin{cases} m_s \ddot{z}_s(t) + c_s [\dot{z}_s(t) - \dot{z}_u(t)] + k_s [z_s(t) - z_u(t)] = u(t) \\ m_u \ddot{z}_u(t) + c_s [\dot{z}_u(t) - \dot{z}_s(t)] + k_s [z_u(t) - z_s(t)] + k_t [z_u(t) - z_r(t)] + c_t [\dot{z}_u(t) - \dot{z}_r(t)] = -u(t) \end{cases} \quad (1)$$

where the symbols are listed in Table 1.

Similar to [11], we evaluate the performance of the ASS from the indicators of ride comfort, road holding and suspension deflection, which is depicted in Table 2.

In Table 2,  $\ddot{z}_s(t)$  in indicator i) is a body acceleration; the indices ii) and iii) are considered from the stroke of mechanical structure points of view and driving stability, respectively.  $z_{max}$  is the given allowable stroke of mechanical structure and  $(m_u + m_s)g$  is the static load, where  $g$  denotes gravitational acceleration [8].

To simplify the representation, we define the following state variables based on the above discussion:

$$\begin{aligned} x_1(t) &= z_s(t) - z_u(t), x_2(t) = z_u(t) - z_r(t), \\ x_3(t) &= \dot{z}_s(t), x_4(t) = \dot{z}_u(t), z_1(t) = \ddot{z}_s(t), \\ z_2(t) &= \left[ \frac{1}{z_{max}} x_1^T(t) \quad \frac{k_t}{(m_s + m_u)g} x_2^T(t) \right]^T. \end{aligned}$$

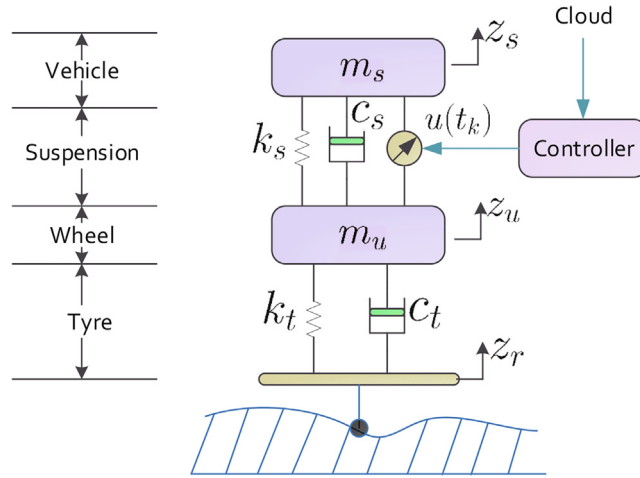


Fig. 1. A cloud-aided quarter-vehicle active suspension system.

Table 1  
Symbols of the ASS

Symbol	Quantity	Symbol	Quantity
$m_s$	sprung mass	$m_u$	unsprung mass
$z_r$	road movement input	$c_s$	damping of suspension
$k_s$	stiffness of suspension system	$k_t$	compressibility of tyre
$c_t$	damping of tyre	$z_s$	movements of sprung masses
$z_u$	movements of unsprung masses	$u$	actuator force
$x_1$	suspension deflection	$x_2$	tyre deflection
$x_3$	sprung mass velocity	$x_4$	unsprung mass velocity

Define  $x(t) = [x_1^T(t) \ x_2^T(t) \ x_3^T(t) \ x_4^T(t)]^T$ , and  $\omega(t) = \dot{z}_r(t)$  which represents the road disturbance, and then the dynamic of the suspension system in (1) can be expressed as

$$\begin{cases} \dot{x}(t) = Ax(t) + Bu(t) + D\omega(t) \\ z_1(t) = C_1x(t) \\ z_2(t) = C_2x(t) \end{cases} \quad (2)$$

where

$$A = \begin{bmatrix} 0 & 0 & 1 & -1 \\ 0 & 0 & 0 & 1 \\ -\frac{k_s}{m_s} & 0 & -\frac{c_s}{m_s} & \frac{c_s}{m_s} \\ \frac{k_s}{m_u} & -\frac{k_t}{m_u} & \frac{c_s}{m_u} & -\frac{c_s+c_t}{m_u} \end{bmatrix},$$

$$B = \begin{bmatrix} 0 & 0 & \frac{1}{m_s} & -\frac{1}{m_u} \end{bmatrix}^T,$$

$$C_1 = \begin{bmatrix} -\frac{k_s}{m_s} & 0 & -\frac{c_s}{m_s} & \frac{c_s}{m_s} \end{bmatrix},$$

$$C_2 = \begin{bmatrix} \frac{1}{z_{max}} & 0 & 0 & 0 \\ 0 & \frac{k_t}{(m_u+m_s)g} & 0 & 0 \end{bmatrix},$$

$$D = \begin{bmatrix} 0 & -1 & 0 & \frac{c_t}{m_u} \end{bmatrix}^T.$$

Taking the fact of the uncertainty of sprung mass ( $m_s(t) \in [m_{smin}, m_{smax}]$ ) into account, we utilize T-S fuzzy modeling approach here by introducing  $\frac{1}{m_s(t)}$  as a premise variable which is denoted by  $\xi(t)$ , i.e.  $\xi(t) \triangleq \frac{1}{m_s(t)}$ .

Define the membership functions  $\mu_1(\xi(t))$  and  $\mu_2(\xi(t))$  as

$$\mu_1(\xi(t)) = \frac{\frac{1}{m_s(t)} - \underline{m}_s}{\overline{m}_s - \underline{m}_s}, \mu_2(\xi(t)) = \frac{\overline{m}_s - \frac{1}{m_s(t)}}{\overline{m}_s - \underline{m}_s}$$

**Table 2**  
Performance evaluation of the ASS

	Indicator	Constraint condition
i)	ride comfort	$\mathbb{E}\{\ \ddot{z}_s(t)\ _2\} < \gamma^2 \mathbb{E}\{\ \omega(t)\ _2\}$
ii)	suspension deflection	$\mathbb{E}\{ z_s(t) - z_u(t) \} \leq z_{max}$
iii)	road holding	$\mathbb{E}\{k_r( z_u(t) - z_r(t) )\} \leq (m_u + m_s)g$

where  $\bar{m}_s = \frac{1}{m_{smin}}$ ,  $\underline{m}_s = \frac{1}{m_{smax}}$ . Obviously,  $\mu_1(\xi(t)) + \mu_2(\xi(t)) = 1$ .

Similar to [11], the suspension system in (2) can be represented by the following T-S fuzzy model:

**Rule i:** IF  $\xi(t)$  is  $\mu_i(\xi(t))$ , THEN

$$\dot{x}(t) = A_i x(t) + B_i u(t) + D\omega(t).$$

Fuzzy blending allows to infer the overall fuzzy model as follows

$$\begin{cases} \dot{x}(t) = \sum_{i=1}^2 \mu_i(\xi(t)) [A_i x(t) + B_i u(t) + D\omega(t)] \\ z_1(t) = \sum_{i=1}^2 \mu_i(\xi(t)) C_{1i} x(t) \\ z_2(t) = \sum_{i=1}^2 \mu_i(\xi(t)) C_{2i} x(t). \end{cases} \tag{3}$$

**Remark 1.** If more physical quantities are considered to be various, for example,  $m_u$  is also a time-varying quantity, the T-S fuzzy model of the system in (2) will extend to be more complicated.

### 2.2. The structure of cloud-aided ASSs

As shown in Fig. 2, the control signal of suspension systems is transmitted over the cloud network which may induce the problem of limited network bandwidth and cyber-attack. In this subsection, a novel memory-based ETM is introduced to mitigate the burden of network bandwidth and deception attacks.

#### 2.2.1. Memory-based ETM

By introducing the ETM, the can save much network communication resources. However, few existed approaches of the ETM use the past information. Before proposing a new memory-based ETM to deal with such a problem, we first give the following definitions for  $m = 1, 2, 3$

$$\begin{aligned} \bar{x}(t_{k-m+1}h) &= \frac{x(t_{k-m+1}h) + x(t_k h)}{2}, \\ e_m(t) &= x(t_{k-m+1}h) - \bar{x}(t_{k-m+1}h), \\ \vartheta_1(t) &= \frac{1}{3} \sum_{m=1}^3 x(t_{k-m+1}h), \\ \vartheta_2(t) &= \sum_{m=1}^3 \lambda_m e_m(t), \\ \vartheta(t) &= \delta_1 \vartheta_1^T(t) \Phi \vartheta_1(t) + \frac{\delta_2}{2} [\vartheta_1^T(t) \Phi \vartheta_2(t) + \vartheta_2^T(t) \Phi \vartheta_1(t)], \\ \psi(t) &= \sum_{m=1}^3 \lambda_m e_m^T(t) \Phi e_m(t) - \vartheta(t) \end{aligned} \tag{4}$$

where  $h$  is a sampling period,  $\{t_k h\}_{k=0}^\infty$  is the monotonic increasing sequence of releasing instants,  $l = 0, 1, 2, \dots$ ,  $\delta_1, \delta_2$  and  $\lambda_m$  are given weighting scalars, and  $\Phi$  is a weighting matrix to be designed. Then the next releasing instant can be defined by

$$t_{k+1}h = t_k h + \max \{(l + 1)h | \psi(t) < 0\} \tag{5}$$

which means that when the event-triggering condition  $\psi(t) < 0$  is invoked, the data-packet at this sampling instant is needed for the control of suspension system, while the packets at instants  $t_k h + lh$  are discarded with  $l = 1, 2, \dots, l_M \triangleq \max_{\psi(t) < 0} \{l\}$  for

$t \in [t_k h, t_{k+1}h)$ .

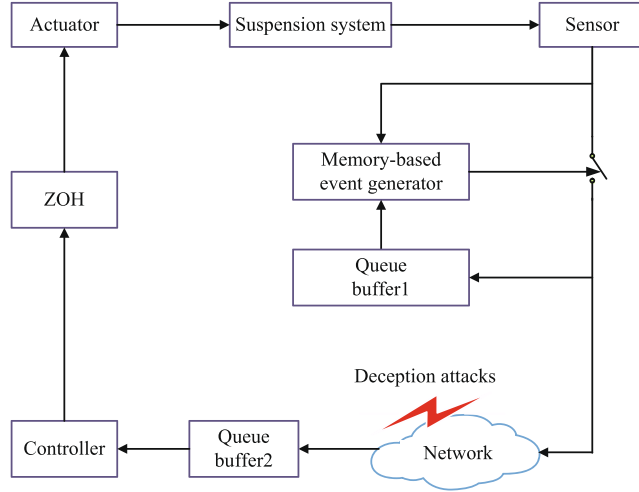


Fig. 2. The structure of the cloud-aided suspension systems.

**Remark 2.** From (4), one can see that the past information  $x(t_{k-m+1}h)$  with  $m = 0, 1, 2$  is used for ETM, which may bring the following advantages: i) the error triggering event arising from accidental abrupt state variation can be mitigated, such as, gross error in measurement; ii) the releasing period can be smoothed.

**Remark 3.** Let  $m = 1$ , the input of ETM will reduce to the memoryless ETM, that is, no historical information is used, while excessive historical information will occupy more computation and memory resources. Therefore, in this study, we select  $m = 3$ .

**Remark 4.** The item  $\frac{\delta_2}{2} [\vartheta_1^T(t)\Phi\vartheta_2(t) + \vartheta_2^T(t)\Phi\vartheta_1(t)]$  in the event-triggering condition can increase the sensibility to deception attacks, thereby leading to a large data-releasing rate during attack periods. Therefore, such an item is useful for getting a better control performance of the system against cyber-attacks.

**Remark 5.** In (4),  $\delta_1$  belongs to  $[0, 1)$ , and  $\delta_2 > 0$  is a weight scalar. If one sets  $m = 1$  and  $\delta_2 = 0$ , the ETM turns to be the traditional ETM, such as the ETM in [28]. If  $\delta_2$  takes a large positive value, small variation of the state within a certain time interval will result in a large average data releasing rate during this period.

### 2.2.2. Fuzzy state feedback control

Taking the memory-based ETM into account, we construct the following fuzzy controller

**Controller Rule j:** IF  $\zeta(t_{k-m+1}h)$  is  $\mu_j^{km}(\zeta(t_{k-m+1}h))$  THEN

$$\bar{u}(t) = K_{jm}x(t_{k-m+1}h)$$

where  $K_{jm}(j \in \{1, 2\}; m \in \{1, 2, 3\})$  are the control gains to be determined.

Then the memory-based fuzzy state feedback control strategy is considered as follows

$$\bar{u}(t) = \sum_{j=1}^2 \sum_{m=1}^3 \mu_j^{km}(\zeta(t_{k-m+1}h)) K_{jm}x(t_{k-m+1}h) \tag{6}$$

for  $t \in [t_k h + \tau_k, t_{k+1} h + \tau_{k+1})$ , where  $\tau_k$  is the network induce delay at instant  $t_k$ .

Similar to [26,16], here, we suppose the membership functions satisfy

$$\mu_j^{km}(\zeta(t_{k-m+1}h)) \geq \rho_j \mu_j(\zeta(t)). \tag{7}$$

For brevity, we define  $\mu_i^i = \mu_i(\zeta(t))$  and  $\mu_j^{km} = \mu_j^{km}(\zeta(t_{k-m+1}h))$  in the next.

The control signal is vulnerable to attack when transmitted over the network. The adversaries inject false data  $f(t)$  into the transmission state, which can be modeled by

$$\tilde{x}(t_k h) = x(t_k h) + f(t_k h) \quad (8)$$

where  $f(t)$  is assumed to satisfy [21]

$$\|M^{\frac{1}{2}}f(t)\|_2 \leq \|Lx(t)\|_2. \quad (9)$$

To avoid being detected from the adversaries point of view, the attack signal is injected in a random way, meanwhile some attack signal fails to inject. Then the real control input is expressed by

$$u(t) = \bar{u}(t) + \sum_{j=1}^2 \sum_{m=1}^3 \alpha(t_{k-m+1}h) K_{jm} f(t_{k-m+1}h) \quad (10)$$

where  $\alpha(t)$  is a random variable satisfying Gaussian distribution with  $\mathbb{E}(\alpha(t)) = \bar{\alpha}$  and  $\text{Var}(\alpha(t)) = \hat{\alpha}$ .

### 2.3. The closed-loop control system of cloud-aided ASSs

Denote  $\tau_k$  with an upper bound  $\bar{\tau}$  as a network-induced delay at  $t_k h$ . It holds that  $[t_k h + \tau_k, t_{k+1} h + \tau_{k+1}) = \bigcup_{l=0}^M \chi_{t_k}^l$  with  $\chi_{t_k}^l = [t_k h + lh + \tau_k, t_{k+1} h + lh + h + \tau_{k+1}^l)$ . We define  $\tau(t) = t - t_k h - lh$  for  $t \in \chi_{t_k}^l$ . It yields that

$$0 \leq \tau(t) \leq h + \bar{\tau} = \tau_M. \quad (11)$$

From the definition (4) and (11), we can obtain

$$x(t_{k-m+1}h) = x(t - \tau(t)) + 2e_m(t). \quad (12)$$

Combining (3), (10) and (12), we get the following closed-loop model of the cloud-aided ASS

$$\begin{cases} \dot{x}(t) = \sum_{i=1}^2 \sum_{j=1}^2 \sum_{m=1}^3 \mu_i^t \mu_j^{km} [A_i x(t) + B_i K_{jm} x(t - \tau(t)) + 2B_i K_{jm} e_m(t) \\ \quad + \alpha(t_{k-m+1}h) B_i K_{jm} f(t_{k-m+1}h) + \omega(t)] \\ z_1(t) = \sum_{i=1}^2 \mu_i^t C_{1i} x(t) \\ z_2(t) = \sum_{i=1}^2 \mu_i^t C_{2i} x(t). \end{cases} \quad (13)$$

Then the main objective of this study is to design a resilient controller for the cloud-aided ASS based on the memory-based ETM, such that the cloud-aided ASS suffering from the false data injection can maintain a certain level of the performance, which is evaluated from the indicators including ride comfort, suspension deflection and road holding (see Table 2).

### 3. Main results

In this section, the resilient controller will be designed for the cloud-aided ASS based on the proposed memory-based ETM. The main purpose of this design is to guarantee the performance of the cloud-aided ASS subject to deception attacks and to decrease the data-releasing rate.

**Theorem 1.** For given positive scalars  $\lambda_m, \tau_M, \rho_i, \rho_j, \bar{\alpha}, \hat{\alpha}$  and  $\delta_i$ , and matrices  $K_{jm}$  with  $i, j \in \{1, 2\}; m \in \{1, 2, 3\}$ , the system (13) is mean square asymptotically stable with  $H_\infty$  norm bound  $\gamma$  and performance indicators i)-iii) in Table 2 can be satisfied as well, if there exist matrices  $P > 0, Q > 0, R > 0, \Phi > 0, \Lambda_i^T = \Lambda_i$  such that

$$\Pi_{ij} - \Lambda_i < 0, \quad (14)$$

$$\rho_i(\Pi_{ii} - \Lambda_i) + \Lambda_i < 0, \quad (15)$$

$$\rho_j(\Pi_{ij} - \Lambda_i) + \Lambda_i + \rho_i(\Pi_{ji} - \Lambda_j) + \Lambda_j < 0 (i < j), \quad (16)$$

$$\begin{bmatrix} -I & * \\ \sqrt{v}\{C_{2i}\}_s^T & -P \end{bmatrix} < 0, (s = 1, 2) \quad (17)$$

$$\mathcal{R} = \begin{bmatrix} \hat{R} & * \\ H & \hat{R} \end{bmatrix} > 0 \quad (18)$$

where

$$\begin{aligned} \Pi_{ij} &= \Pi_{ij}^1 + \Pi_{ij}^2, \Pi_{ij}^1 = \left[ \Psi^{ij} \right]_{12 \times 12}, \Psi_{11}^{ij} = A_i^T P + PA_i + Q - 4R, \\ \Psi_{21}^{ij} &= \sum_{m=1}^3 \left( K_{jm}^T B_i^T P \right) - 2R - H_1 - H_2 - H_2^T - H_3, \\ \Psi_{22}^{ij} &= \delta_1 \Phi - 8R + H_1^T + H_1 - H_3^T - H_3, \\ \Psi_{31}^{ij} &= H_1 - H_2 + H_2^T - H_3^T, \Psi_{32}^{ij} = -2R - H_1 + H_2^T + H_2 - H_3, \Psi_{33}^{ij} = -Q - 4R, \\ \Psi_{(m+3)1}^{ij} &= K_{jm}^T B_i^T P, \Psi_{(m+3)2}^{ij} = \sigma_{1m} \Phi, \Psi_{(m+3)(m+3)}^{ij} = \sigma_{2m} \Phi, \\ \Psi_{54}^{ij} &= \sigma_3 \Phi, \Psi_{64}^{ij} = \sigma_4 \Phi, \Psi_{65}^{ij} = \sigma_5 \Phi, \Psi_{71}^{ij} = 6R, \Psi_{72}^{ij} = 6R + 2H_2 + 2H_3^T, \\ \Psi_{73}^{ij} &= -2H_2 + 2H_3^T, \Psi_{77}^{ij} = \Psi_{88}^{ij} = -12R, \Psi_{81}^{ij} = 2H_2 + H_3, \\ \Psi_{82}^{ij} &= 6R - 2H_2 + 2H_3, \Psi_{83}^{ij} = 6R, \Psi_{87}^{ij} = -4H_3, \\ \Psi_{(m+8)1}^{ij} &= \bar{\alpha} K_{jm}^T B_i^T P, \Psi_{(m+8)(m+8)}^{ij} = -M, \Psi_{121}^{ij} = D^T P, \Psi_{1212}^{ij} = -\gamma^2 I, \\ \sigma_{1m} &= \frac{2}{3} \delta_1 + \frac{1}{2} \delta_2 \lambda_m, \sigma_{2m} = \frac{4}{9} \delta_1 + \frac{2}{3} \delta_2 \lambda_m - \lambda_m, \sigma_3 = \frac{4}{9} \delta_1 + \frac{1}{3} \delta_2 \lambda_1 + \frac{1}{3} \delta_2 \lambda_2, \\ \sigma_4 &= \frac{4}{9} \delta_1 + \frac{1}{3} \delta_2 \lambda_1 + \frac{1}{3} \delta_2 \lambda_3, \sigma_5 = \frac{4}{9} \delta_1 + \frac{1}{3} \delta_2 \lambda_2 + \frac{1}{3} \delta_2 \lambda_3, \\ \Pi_{ij}^2 &= \tau_M^2 A_i^T R A + \tau_M^2 B_i^T R B + C^T C + D^T D, \\ A &= \left[ A_i \sum_{m=1}^3 B_i K_{jm} O B_i K_{j1} B_i K_{j2} B_i K_{j3} 0 0 \bar{\alpha} B_i K_{j1} \bar{\alpha} B_i K_{j2} \bar{\alpha} B_i K_{j3} D \right], \\ B &= \left[ 0 \dots 0 \hat{\alpha} B_i K_{j1} \hat{\alpha} B_i K_{j2} \hat{\alpha} B_i K_{j3} 0 \right], \hat{R} = \begin{bmatrix} R & 0 \\ 0 & 3R \end{bmatrix}, \\ C &= \left[ C_{1i} 0 \dots 0 \right], D = \left[ \sqrt{3} L 0 \dots 0 \right], H = \begin{bmatrix} H_1 & * \\ H_2 & H_3 \end{bmatrix}. \end{aligned}$$

**Proof.** Construct the following Lyapunov-Krasovskii functional

$$V(t) = x^T(t) P x(t) + \int_{t-\tau_M}^t x^T(s) Q x(s) ds + \tau_M \int_{t-\tau_M}^t \int_s^t \dot{x}^T(v) R \dot{x}(v) dv ds \tag{19}$$

Then we have

$$\begin{aligned} \mathbb{E} \left\{ \dot{V}(t) \right\} &\leq \mathbb{E} \left\{ 2x^T(t) P \dot{x}(t) + x^T(t) Q x(t) - x^T(t - \tau_M) Q x(t - \tau_M) \right. \\ &\quad \left. + \tau_M^2 \dot{x}^T(t) R \dot{x}(t) - \tau_M \int_{t-\tau_M}^t \dot{x}^T(s) R \dot{x}(s) ds \right\} \end{aligned} \tag{20}$$

Recalling the memory-based ETM in (4) and the constrain of cyber-attacks in (9) yields that

$$\begin{aligned} \mathbb{E} \left\{ \dot{V}(t) \right\} &\leq \mathbb{E} \left\{ 2x^T(t) P \dot{x}(t) + x^T(t) Q x(t) - x^T(t - \tau_M) Q x(t - \tau_M) \right. \\ &\quad \left. + \tau_M^2 \dot{x}^T(t) R \dot{x}(t) - \tau_M \int_{t-\tau_M}^t \dot{x}^T(s) R \dot{x}(s) ds - \sum_{m=1}^3 \lambda_m e_m^T(t) \Phi e_m(t) + \vartheta^T(t) \right. \\ &\quad \left. - \sum_{m=1}^3 \left[ f^T(t_{k-m+1} h) M f(t_{k-m+1} h) - x^T(t) L^T L x(t) \right] + z_1^T(t) z_1(t) - \gamma^2 \omega^T(t) \omega(t) \right\}. \end{aligned} \tag{21}$$

For convenience of description, we denote

$$\zeta(t) = \left[ x^T(t) \ x^T(t - \tau(t)) \ x^T(t - \tau_M) \zeta_e^T(t) \zeta_{w1}^T(t) \ \zeta_{w2}^T(t) \zeta_f^T(t) \ \omega^T(t) \right]^T,$$

where  $\zeta_e^T(t) = [e_1^T(t) \ e_2^T(t) \ e_3^T(t)]$ ,  $\zeta_{w1}^T(t) = \frac{1}{\tau(t)} \int_{t-\tau(t)}^t x^T(s) ds$ ,  $\zeta_{w2}^T(t) = \frac{1}{\tau_M - \tau(t)} \int_{t-\tau_M}^{t-\tau(t)} x^T(s) ds$ , and  $\zeta_f^T(t) = [f^T(t_k h) \ f^T(t_{k-1} h) \ f^T(t_{k-2} h)]$ .

Notice that  $\mathbb{E}\{\bar{\alpha} - \alpha(t)\} = 0$ ,  $\mathbb{E}\{(\bar{\alpha} - \alpha(t))^2\} = \hat{\alpha}^2$ , we can obtain that

$$\mathbb{E} \left\{ \dot{x}^T(t) R \dot{x}(t) \right\} = \sum_{i=1}^2 \sum_{j=1}^2 \mu_i^i \mu_j^{km} \zeta^T(t) \left( A^T R A + B^T R B \right) \zeta(t). \tag{22}$$

Define

$$T_1 = [I - \underbrace{I0 \dots 0}_{10}], T_2 = [\underbrace{I0 \dots 0}_4 - 2\underbrace{I0 \dots 0}_5], T_3 = [0I - \underbrace{I0 \dots 0}_9],$$

$$T_4 = [0\underbrace{I0 \dots 0}_4 - 2\underbrace{I0 \dots 0}_4], \Omega_i = T_i \zeta(t), (i = 1, 2, 3, 4), \hat{\Omega}_1 = \begin{bmatrix} \Omega_1 \\ \Omega_2 \end{bmatrix}, \hat{\Omega}_2 = \begin{bmatrix} \Omega_3 \\ \Omega_4 \end{bmatrix}.$$

Applying the Wirtinger-based inequality in [18], the following inequalities are hold

$$-\tau_M \int_{t-\tau(t)}^t \dot{x}^T(s)R\dot{x}(s)ds \leq -\frac{\tau_M}{\tau(t)} \hat{\Omega}_1^T \begin{bmatrix} R & 0 \\ 0 & 3R \end{bmatrix} \hat{\Omega}_1, \tag{23}$$

$$-\tau_M \int_{t-\tau_M}^{t-\tau(t)} \dot{x}^T(s)R\dot{x}(s)ds \leq -\frac{\tau_M}{\tau_M - \tau(t)} \hat{\Omega}_2^T \begin{bmatrix} R & 0 \\ 0 & 3R \end{bmatrix} \hat{\Omega}_2. \tag{24}$$

Using the similar method in [17] for (23) and (24) follows that

$$\begin{aligned} -\tau_M \int_{t-\tau_M}^t \dot{x}^T(s)R\dot{x}(s)ds &= -\tau_M \int_{t-\tau(t)}^t \dot{x}^T(s)R\dot{x}(s)ds - \tau_M \int_{t-\tau_M}^{t-\tau(t)} \dot{x}^T(s)R\dot{x}(s)ds \\ &\leq -\begin{bmatrix} \hat{\Omega}_1 \\ \hat{\Omega}_2 \end{bmatrix}^T \begin{bmatrix} \frac{\tau_M}{\tau(t)} \hat{R} & 0 \\ 0 & \frac{\tau_M}{\tau_M - \tau(t)} \hat{R} \end{bmatrix} \begin{bmatrix} \hat{\Omega}_1 \\ \hat{\Omega}_2 \end{bmatrix} \\ &\leq -\begin{bmatrix} \hat{\Omega}_1 \\ \hat{\Omega}_2 \end{bmatrix}^T \mathcal{R} \begin{bmatrix} \hat{\Omega}_1 \\ \hat{\Omega}_2 \end{bmatrix} \end{aligned} \tag{25}$$

Combining (21), (22) and (25) has

$$\mathbb{E}\{\dot{V}(t)\} \leq \mathbb{E}\left\{ \sum_{i=1}^2 \sum_{j=1}^2 \mu_i^t \mu_j^{km} \zeta^T(t) \Pi_{ij} \zeta(t) \right\}. \tag{26}$$

Similar to the method of dealing with the problem of asynchronisation of premise variables in [12], for  $\Lambda_i^T = \Lambda_i$  we have

$$\begin{aligned} \mathbb{E}\left\{ \sum_{i=1}^2 \sum_{j=1}^2 \mu_i^t \mu_j^{km} \zeta^T(t) \Pi_{ij} \zeta(t) \right\} &\leq \mathbb{E}\left\{ \sum_{i=1}^2 \sum_{j=1}^2 \mu_i^t \mu_j^t \zeta^T(t) [\rho_i (\Pi_{ii} - \Lambda_i) + \Lambda_i] \zeta(t) \right. \\ &\quad \left. + \sum_{i=1}^2 \sum_{i < j} \mu_i^t \mu_j^t \zeta^T(t) [\rho_j (\Pi_{ij} - \Lambda_i) + \rho_i (\Pi_{ji} - \Lambda_j) + \Lambda_i + \Lambda_j] \zeta(t) \right\}. \end{aligned} \tag{27}$$

So far, one can know that (14)–(16) are sufficient conditions to ensure

$$\mathbb{E}\{\dot{V}(t) + z_1^T(t)z_1(t) - \gamma^2 \omega^T(t)\omega(t)\} < 0 \tag{28}$$

Under the zero initial condition, one can get  $\mathbb{E}\{z_1^T(t)z_1(t) - \omega^T(t)\omega(t)\} < 0$  for  $\omega(t) \neq 0$ , which guarantees the performance indicator i) in Table 2. For  $\omega(t) = 0$ , it follows  $\mathbb{E}\{\dot{V}(t)\} < 0$  from (28), which guarantees the networked ASS is mean square asymptotically stable.

Define  $v = \inf_{t>0} \left\{ V(0) + \int_0^t [z_1^T(t)z_1(t) - \gamma^2 \omega^T(t)\omega(t)] dt \right\}$ . From (19) and (28), one can obtain that

$$x^T(t)Px(t) \leq v. \tag{29}$$

For convenience of representation, we use  $\{z_2(t)\}_s$  and  $\{C_{2i}\}_s$  to denote the  $s$ -th line of matrix  $z_2(t)$  and  $C_{2i}$ , respectively. For  $s = 1, 2$ , from (29) it yields that

$$\begin{aligned} \sum_{i=1}^2 \mu_i^t [x^T(t) \{C_{2i}\}_s^T \{C_{2i}\}_s x(t)] &= \sum_{i=1}^2 \mu_i^t [x^T(t) P^{\frac{1}{2}} P^{-\frac{1}{2}} \{C_{2i}\}_s^T \{C_{2i}\}_s P^{-\frac{1}{2}} P^{\frac{1}{2}} x(t)] \\ &\leq \lambda_{\max} \left\{ \sum_{i=1}^2 \mu_i^t [P^{-\frac{1}{2}} \{C_{2i}\}_s^T \{C_{2i}\}_s P^{-\frac{1}{2}}] \right\} x^T(t)Px(t) \\ &\leq \lambda_{\max} \left\{ \sum_{i=1}^2 \mu_i^t [v P^{-\frac{1}{2}} \{C_{2i}\}_s^T \{C_{2i}\}_s P^{-\frac{1}{2}}] \right\} \end{aligned} \tag{30}$$

where  $\lambda_{\max}\{\cdot\}$  represents the maximal eigenvalue.

By using Schur complement to (17), it follows that

$$v P^{-\frac{1}{2}} \{C_{2i}\}_s^T \{C_{2i}\}_s P^{-\frac{1}{2}} \leq I (s = 1, 2). \tag{31}$$

Combining (30) and (31), for  $s = 1, 2$  one can obtain

$$\max_{t>0} |z_2(t)|_s^2 \leq \max_{t>0} \left\| \sum_{i=1}^2 \mu_i^t \left[ x^T(t) \{C_{2i}\}_s^T \{C_{2i}\}_s x(t) \right] \right\|_2 \leq I \tag{32}$$

which ensures the performance ii) and iii) in Table 2. The proof is completed.

**Remark 6.** Theorem 1 presents a sufficient condition such that the system (13) is mean square asymptotically stable with an  $H_\infty$  norm bound  $\gamma$ . It is based on the simple Lyapunov-Krasovskii functional (LKF) (19). If we replace the LKF with a new one as that in [34], a better condition can be derived, but it may be more complicated.

**Theorem 2.** For given positive scalars  $\lambda_m, \tau_M, \rho_i, \rho_j, \bar{\alpha}, \hat{\alpha}, \delta_i$  and  $\varepsilon$ , the system (13) is mean square asymptotically stable with  $H_\infty$  norm bound  $\gamma$  and performance indicators i)-iii) in Table 2 can be satisfied as well, if there exist matrices  $X > 0, \tilde{R} > 0, \tilde{M} > 0, \tilde{\Phi} > 0, \tilde{\Lambda}_i^T = \tilde{\Lambda}_i$  with  $i, j \in \{1, 2\}; m \in \{1, 2, 3\}$  such that

$$\begin{bmatrix} \Xi_1^{ij} & * & * & * & * \\ c\tau_M \tilde{A} & \Xi & * & * & * \\ \tau_M \tilde{B} & 0 & \Xi & * & * \\ \tilde{C} & 0 & 0 & -I & * \\ \tilde{D} & 0 & 0 & 0 & -I \end{bmatrix} < 0, \tag{33}$$

$$\begin{bmatrix} \Xi_2^{ij} & * & * & * & * \\ \tau_M \tilde{A} & \Xi & * & * & * \\ \tau_M \tilde{B} & 0 & \Xi & * & * \\ \tilde{C} & 0 & 0 & -I & * \\ \tilde{D} & 0 & 0 & 0 & -I \end{bmatrix} < 0, \tag{34}$$

$$\begin{bmatrix} \Xi_3^{ij} & * & * & * & * \\ \tau_M \tilde{A} & \Xi & * & * & * \\ \tau_M \tilde{B} & 0 & \Xi & * & * \\ \tilde{C} & 0 & 0 & -I & * \\ \tilde{D} & 0 & 0 & 0 & -I \end{bmatrix} < 0 (i < j), \tag{35}$$

$$\begin{bmatrix} -I & * \\ \sqrt{\nu} X \{C_{2i}\}_s^T & -X \end{bmatrix} < 0, (s = 1, 2) \tag{36}$$

$$\tilde{\mathcal{R}} = \begin{bmatrix} \tilde{R} & * \\ \tilde{H} & \tilde{R} \end{bmatrix} > 0. \tag{37}$$

where

$$\Xi = \varepsilon^2 \tilde{R} - 2\varepsilon X, \Xi_1^{ij} = \tilde{\Psi}^{ij} - \tilde{\Lambda}_i, \Xi_2^{ij} = \rho_i (\tilde{\Psi}^{ii} - \tilde{\Lambda}_i) + \tilde{\Lambda}_i,$$

$$\Xi_3^{ij} = \rho_j (\tilde{\Psi}^{ij} - \tilde{\Lambda}_i) + \tilde{\Lambda}_i + \rho_i (\tilde{\Psi}^{ij} - \tilde{\Lambda}_j) + \tilde{\Lambda}_j,$$

$$[\tilde{\Psi}^{ij}]_{12 \times 12}, \tilde{\Psi}_{11}^{ij} = XA_i^T + A_i X + \tilde{Q} - 4\tilde{R},$$

$$\tilde{\Psi}_{21}^{ij} = \sum_{m=1}^3 (Y_{jm}^T B_m^T) - 2\tilde{R} - \tilde{H}_1 - \tilde{H}_2 - \tilde{H}_2^T - \tilde{H}_3,$$

$$\tilde{\Psi}_{22}^{ij} = \delta_1 \tilde{\Phi} - 8\tilde{R} + \tilde{H}_1^T + \tilde{H}_1 - \tilde{H}_3^T - \tilde{H}_3,$$

$$\tilde{\Psi}_{31}^{ij} = \tilde{H}_1 - \tilde{H}_2 + \tilde{H}_2^T - \tilde{H}_3^T, \tilde{\Psi}_{32}^{ij} = -2\tilde{R} - \tilde{H}_1 + \tilde{H}_2^T + \tilde{H}_2 - \tilde{H}_3, \tilde{\Psi}_{33}^{ij} = -\tilde{Q} - 4\tilde{R},$$

$$\tilde{\Psi}_{(m+3)1}^{ij} = Y_{jm}^T B_m^T, \tilde{\Psi}_{(m+3)2}^{ij} = \sigma_{1m} \tilde{\Phi}, \tilde{\Psi}_{(m+3)(m+3)}^{ij} = \sigma_{2m} \tilde{\Phi},$$

$$\begin{aligned}
 \tilde{\Psi}_{54}^{ij} &= \sigma_3 \tilde{\Phi}, \tilde{\Psi}_{64}^{ij} = \sigma_4 \tilde{\Phi}, \tilde{\Psi}_{65}^{ij} = \sigma_5 \tilde{\Phi}, \tilde{\Psi}_{71}^{ij} = 6\tilde{R}, \tilde{\Psi}_{72}^{ij} = 6\tilde{R} + 2\tilde{H}_2 + 2\tilde{H}_3^T, \\
 \tilde{\Psi}_{73}^{ij} &= -2\tilde{H}_2 + 2\tilde{H}_3^T, \tilde{\Psi}_{77}^{ij} = \tilde{\Psi}_{88}^{ij} = -12\tilde{R}, \tilde{\Psi}_{81}^{ij} = 2\tilde{H}_2 + \tilde{H}_3, \\
 \tilde{\Psi}_{82}^{ij} &= 6\tilde{R} - 2\tilde{H}_2 + 2\tilde{H}_3, \tilde{\Psi}_{83}^{ij} = 6\tilde{R}, \tilde{\Psi}_{87}^{ij} = -4\tilde{H}_3, \\
 \tilde{\Psi}_{(m+8)1}^{ij} &= \tilde{\alpha} Y_{jm}^T B_i^T, \tilde{\Psi}_{(m+8)(m+8)}^{ij} = -\tilde{M}, \tilde{\Psi}_{121}^{ij} = D^T, \tilde{\Psi}_{1212}^{ij} = -\gamma^2 I, \\
 \tilde{A} &= \left[ A_i X \sum_{m=1}^3 B_i Y_{jm} O B_i Y_{j1} B_i Y_{j2} B_i Y_{j3} O O \tilde{\alpha} B_i Y_{j1} \tilde{\alpha} B_i Y_{j2} \tilde{\alpha} B_i Y_{j3} D \right], \\
 \tilde{B} &= \left[ \underbrace{0 \dots 0}_{8} \tilde{\alpha} B_i Y_{j1} \tilde{\alpha} B_i Y_{j2} \tilde{\alpha} B_i Y_{j3} 0 \right], \tilde{R} = \begin{bmatrix} \tilde{R} & 0 \\ 0 & 3\tilde{R} \end{bmatrix}, \\
 \tilde{C} &= \left[ C_{1i} X \underbrace{0 \dots 0}_{11} \right], \tilde{D} = \left[ \sqrt{3} L X \underbrace{0 \dots 0}_{11} \right], \tilde{H} = \begin{bmatrix} \tilde{H}_1 & * \\ \tilde{H}_2 & \tilde{H}_3 \end{bmatrix}.
 \end{aligned}$$

Moreover, the proposed controller feedback gain can be computed as  $K_{jm} = Y_{jm} X^{-1}, \Phi = X^{-1} \tilde{\Phi} X^{-1}$ .

**Proof.** Define  $X = P^{-1}, J_1 = \text{diag}\{X, \dots, X_{11}, I\}, J_2 = \text{diag}\{X, X, I, I\}, J = \text{diag}\{J_1, J_2\}$ , and  $\tilde{\Phi} = X\Phi X, \tilde{H}_1 = XH_1 X, \tilde{H}_2 = XH_2^T X, \tilde{H}_3 = XH_3^T X, \tilde{H} = \begin{bmatrix} \tilde{H}_1 & * \\ \tilde{H}_2 & \tilde{H}_3 \end{bmatrix}, \tilde{R} = XRX, \tilde{R} = \begin{bmatrix} \tilde{R} & 0 \\ 0 & 3\tilde{R} \end{bmatrix}, \tilde{Q} = XQX, \tilde{M} = XMX, Y_{jm} = K_{jm} X$ .

Using Schur complement to (14) yields that

$$\begin{bmatrix} \Psi^{ij} - \Lambda_i & * & * & * & * \\ \tau_M \tilde{A} & -R^{-1} & * & * & * \\ \tau_M \tilde{B} & 0 & -R^{-1} & * & * \\ \tilde{C} & 0 & 0 & -I & * \\ \tilde{D} & 0 & 0 & 0 & -I \end{bmatrix} < 0 \tag{38}$$

Notice that

$$-PR^{-1}P \leq -2\varepsilon P + \varepsilon^2 R \tag{39}$$

It can be concluded that (33) is a sufficient condition to ensure (38) holds from (39) and pre- and post-multiplying (38) with  $J$ . Similarly, we can obtain (34), (35), (36) and (37). This completes the proof.

As stated in Remark 5, by selecting  $m = 1$  and  $\delta_2 = 0$ , the memory-based ETM can be degenerated into a traditional memoryless ETM. Similar to Theorem 2, we can obtain the following results.

**Corollary 1.** For given positive scalars  $\tau_M, \rho_i, \rho_j, \tilde{\alpha}, \hat{\alpha}, \delta$  and  $\varepsilon$ , the system (13) is mean square asymptotically stable with an  $H_\infty$  norm bound  $\gamma$  and performance indicators i)-iii) in Table 2 can be satisfied as well, if there exist matrices  $X > 0, \tilde{Q} > 0, \tilde{R} > 0, \tilde{M} > 0, \tilde{\Phi} > 0, \tilde{\Lambda}_i^T = \tilde{\Lambda}_j$  with  $i, j \in \{1, 2\}$  such that

$$\begin{bmatrix} \Xi_1^{ij} & * & * & * & * \\ \tau_M \tilde{A} & \Xi & * & * & * \\ \tau_M \tilde{B} & 0 & \Xi & * & * \\ \tilde{C} & 0 & 0 & -I & * \\ \tilde{D} & 0 & 0 & 0 & -I \end{bmatrix} < 0, \tag{40}$$

$$\begin{bmatrix} \Xi_2^{ij} & * & * & * & * \\ \tau_M \tilde{A} & \Xi & * & * & * \\ \tau_M \tilde{B} & 0 & \Xi & * & * \\ \tilde{C} & 0 & 0 & -I & * \\ \tilde{D} & 0 & 0 & 0 & -I \end{bmatrix} < 0, \tag{41}$$

$$\begin{bmatrix} \Xi_3^{ij} & * & * & * & * \\ \tau_M \tilde{A} & \Xi & * & * & * \\ \tau_M \tilde{B} & 0 & \Xi & * & * \\ \tilde{C} & 0 & 0 & -I & * \\ \tilde{D} & 0 & 0 & 0 & -I \end{bmatrix} < 0, (i < j) \tag{42}$$

$$\begin{bmatrix} -I & * \\ \sqrt{\nu} X \{C_{2i}\}_s^T & -X \end{bmatrix} < 0, (s = 1, 2) \tag{43}$$

$$\tilde{\mathcal{R}} = \begin{bmatrix} \tilde{R} & * \\ \tilde{H} & \tilde{R} \end{bmatrix} > 0. \tag{44}$$

where

$$\begin{aligned} \Xi &= \varepsilon^2 \tilde{R} - 2\varepsilon X, \Xi_1^{ij} = \tilde{\Psi}^{ij} - \tilde{\Lambda}_i, \Xi_2^{ij} = \rho_i (\tilde{\Psi}^{ii} - \tilde{\Lambda}_i) + \tilde{\Lambda}_i, \\ \Xi_3^{ij} &= \rho_j (\tilde{\Psi}^{jj} - \tilde{\Lambda}_j) + \tilde{\Lambda}_i + \rho_i (\tilde{\Psi}^{ij} - \tilde{\Lambda}_j) + \tilde{\Lambda}_j, \\ [\tilde{\Psi}^{ij}]_{12 \times 12}, \tilde{\Psi}_{11}^{ij} &= X A_i^T + A_i X + \tilde{Q} - 4\tilde{R}, \\ \tilde{\Psi}_{21}^{ij} &= Y_j^T B_i^T - 2\tilde{R} - \tilde{H}_1 - \tilde{H}_2 - \tilde{H}_2^T - \tilde{H}_3, \\ \tilde{\Psi}_{22}^{ij} &= \delta \tilde{\Phi} - 8\tilde{R} + \tilde{H}_1^T + \tilde{H}_1 - \tilde{H}_3^T - \tilde{H}_3, \\ \tilde{\Psi}_{31}^{ij} &= \tilde{H}_1 - \tilde{H}_2 + \tilde{H}_2^T - \tilde{H}_3^T, \tilde{\Psi}_{32}^{ij} = -2\tilde{R} - \tilde{H}_1 + \tilde{H}_2^T + \tilde{H}_2 - \tilde{H}_3, \\ \tilde{\Psi}_{33}^{ij} &= -\tilde{Q} - 4\tilde{R}, \tilde{\Psi}_{41}^{ij} = Y_j^T B_i^T, \tilde{\Psi}_{42}^{ij} = 2\delta \tilde{\Phi}, \tilde{\Psi}_{44}^{ij} = 4\delta \tilde{\Phi} - \tilde{\Phi}, \\ \tilde{\Psi}_{51}^{ij} &= 6\tilde{R}, \tilde{\Psi}_{52}^{ij} = 6\tilde{R} + 2\tilde{H}_2 + 2\tilde{H}_3^T, \tilde{\Psi}_{53}^{ij} = -2\tilde{H}_2 + 2\tilde{H}_3^T, \\ \tilde{\Psi}_{55}^{ij} &= \tilde{\Psi}_{66}^{ij} = -12\tilde{R}, \tilde{\Psi}_{61}^{ij} = 2\tilde{H}_2 + \tilde{H}_3, \tilde{\Psi}_{62}^{ij} = 6\tilde{R} - 2\tilde{H}_2 + 2\tilde{H}_3, \\ \tilde{\Psi}_{63}^{ij} &= 6\tilde{R}, \tilde{\Psi}_{65}^{ij} = -4\tilde{H}_3, \tilde{\Psi}_{71}^{ij} = \alpha Y_j^T B_i^T, \tilde{\Psi}_{77}^{ij} = -\tilde{M}, \\ \tilde{\Psi}_{81}^{ij} &= D^T, \tilde{\Psi}_{88}^{ij} = -\gamma^2 I, \tilde{\mathcal{A}} = [A_i X B_i Y_j O B_i Y_j O O \alpha B_i Y_j D], \\ \tilde{\mathcal{B}} &= [0 \dots 0 \alpha B_i Y_j 0], \tilde{\mathcal{C}} = [C_{1i} X O \dots O], \\ \tilde{\mathcal{D}} &= [L X O \dots O], \tilde{H} = \begin{bmatrix} \tilde{H}_1 & * \\ \tilde{H}_2 & \tilde{H}_3 \end{bmatrix}, \tilde{R} = \begin{bmatrix} \tilde{R} & 0 \\ 0 & 3\tilde{R} \end{bmatrix}. \end{aligned}$$

Moreover, the proposed controller feedback gain can be computed as  $K_j = Y_j X^{-1}, \Phi = X^{-1} \tilde{\Phi} X^{-1}$ .

### 4. Simulation

In this section, the proposed method is applied to the model of the ASS in [11] to manifest its advantage. The sprung mass  $m_s$  varies from 230 kg to 470 kg and the other nominal parameters of the ASS are listed in Table 3.

A shock road profile is considered in this example, which is a kind of discrete event with short time and high intensity. It can be modeled by

$$z_r(t) = \begin{cases} \frac{A}{2} (1 - \cos(\frac{2\pi V_0}{l} t)), & 0 \leq t \leq \frac{l}{V_0} \\ 0, & t > \frac{l}{V_0} \end{cases} \tag{45}$$

where  $A$  and  $l$  refer to the height and length of the bump respectively. Here we select  $A = 0.06m, l = 5m, V_0 = 45km/h$ .

Suppose the sampling period  $h = 0.01s, \gamma = 5, \delta_1 = 0.01, \lambda_1 = 0.5, \lambda_2 = 0.3, \lambda_3 = 0.2, \tilde{\alpha} = 0.1, \hat{\alpha} = 0.1, L = 0.5I, \rho_1 = 1.05, \rho_2 = 1.01, \varepsilon = 0.1$ , and evaluation parameters  $z_{max} = 0.03, \tau_M = 0.1$ .

To demonstrate the superiority of our proposed memory-based ETM, in the following, three cases listed in Table 4 are studied.

**Table 3**  
Nominal parameters of the ASS

$m_u(kg)$	$k_s(kN/m)$	$c_s(kNs/m)$	$k_t(kN/m)$	$c_t(Ns/m)$
100	30	1.2	200	160

**Table 4**  
Three cases for memory-based ETM

Case	$m$	$\delta_2$	attack period	Data releasing rate
i)	1	0	0-5s	46.10% (0-5s)
ii)	3	0.1	0-5s	56.80% (0-5s)
iii)	3	0.1	3-4s	60.00% (3-4s)
	3	0.1	3-4s	52.00% (4-5s)

**Case i):** The ETM is degenerated into a memoryless ETM with  $m = 1$  and  $\delta_2 = 0$  (the general ETM). By using [Corollary 1](#), we can get

$$\Phi = 10^3 \times \begin{bmatrix} 0.9730 & -0.0104 & 0.0383 & -0.0387 \\ -0.0104 & 1.2816 & 0.0032 & -0.0091 \\ 0.0383 & 0.0032 & 0.0016 & -0.0016 \\ -0.0387 & -0.0091 & -0.0016 & 0.0016 \end{bmatrix}, \tag{46}$$

$$K_1 = 10^2 \times [0.5539 \quad 9.0675 \quad -1.7368 \quad 1.1312],$$

$$K_2 = 10^2 \times [0.1288 \quad 3.9748 \quad -1.9035 \quad 0.2272].$$

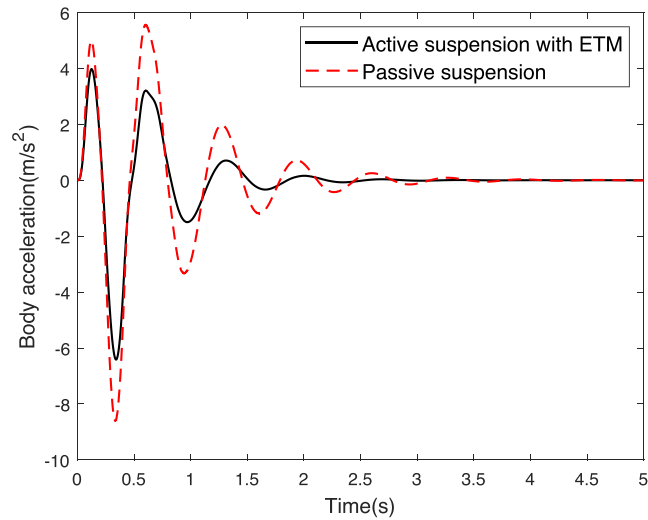


**Fig. 3.** Body acceleration.

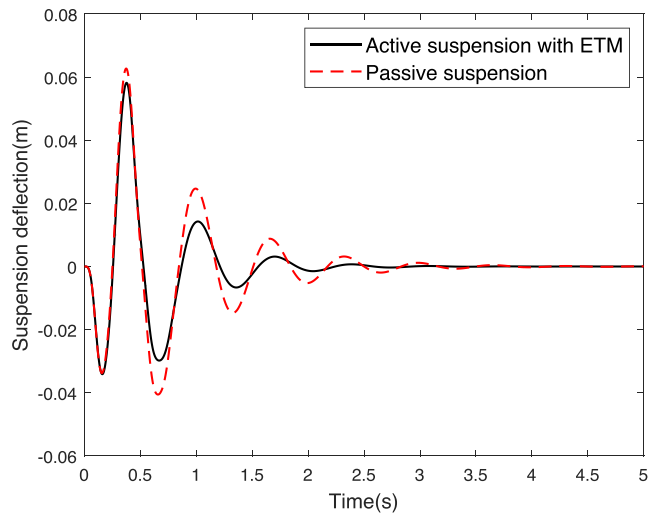


**Fig. 4.** Suspension deflection.

It should be noted that [Corollary 1](#) is derived based on the lemma of Wirtinger's inequality which can lead to less conservative results. By using [Corollary 1](#), the minimum of  $\gamma$  is 1.7569, while the minimum of  $\gamma$  is 4.5127 when using the method based on Jessen inequality in [\[11\]](#).

The black solid lines in [Fig. 3–5](#) plot the responses of body acceleration, suspension deflection and the tyre deflection, respectively under [\(46\)](#), from which one can see indicators in [Table 2](#) can be ensured to a certain lever under the shock road profile and random cyber-attacks. One can obviously see that indicators of the networked ASS in [Table 2](#) by using the general ETM are better than that of the passive suspension which are plotted with red dash lines in [Fig. 3–5](#). The releasing time-sequence depicted in [Fig. 6](#) proves that many data packets are discarded by this kind of ETM. see [Fig. 4](#)

**Case ii):** This case utilizes the proposed memory-based ETM in this study by setting  $m = 3$  and  $\delta_2 = 0.1$ . Using [Theorem 2](#) follows that

$$\Phi = 10^3 \times \begin{bmatrix} 3.0935 & -0.3092 & 0.1199 & -0.1206 \\ -0.3092 & 4.8917 & -0.0022 & -0.0246 \\ 0.1199 & -0.0022 & 0.0050 & -0.0048 \\ -0.1206 & -0.0246 & -0.0048 & 0.0052 \end{bmatrix},$$

$$K_{11} = 10^2 \times [0.4900 \quad 3.6494 \quad -0.7576 \quad 0.4145],$$

$$K_{12} = 10^2 \times [0.6139 \quad 3.8605 \quad -0.7103 \quad 0.4718],$$

$$K_{13} = 10^2 \times [0.4922 \quad 3.0093 \quad -0.5487 \quad 0.3769],$$

$$K_{21} = 10^2 \times [0.0484 \quad 1.6545 \quad -0.9108 \quad 0.0822],$$

$$K_{22} = 10^2 \times [0.0342 \quad 0.9318 \quad -0.5309 \quad 0.0478],$$

$$K_{23} = 10^2 \times [0.0297 \quad 0.5580 \quad -0.3343 \quad 0.0301].$$
(47)

The blue solid lines in [Fig. 7–9](#) present the responses of body acceleration, suspension deflection and tyre deflection, respectively under [\(47\)](#). Furthermore, it can be seen that the performance of the networked ASS using the memory-based ETM is better than that of the networked ASS using the general ETM, where the black dash lines are the responses of networked ASSs using the general ETM (Case i). [Fig. 6](#) and [Fig. 10](#) show that the average data releasing rate 0-5s of the networked ASS with memory-based ETM is higher than the one with the general ETM, that is to say, the system with memory-based ETM receives more data for getting a better performance when the system subject to deception attacks and road disturbance. Moreover, the memory-based ETM in Case ii) is more sensitive for deception attacks and road disturbance than general ETM in Case i), which is contributed to the item  $\frac{\delta_2}{2} [\vartheta_1^T(t)\Phi\vartheta_2(t) + \vartheta_2^T(t)\Phi\vartheta_1(t)]$  in the proposed memory-based ETM. see [Fig. 8](#)

**Case iii):** To better manifest the sensitivity of memory-based ETM for deception attacks, we suppose the random deception attacks only occur during 3–4s.

[Fig. 11](#) and [Table 4](#) show the releasing time-sequence under this scenario, from which one can see clearly that the average data releasing rate during 3–4s is much higher than the one during 4–5s, which leads to a better control performance of the system against deception attacks.

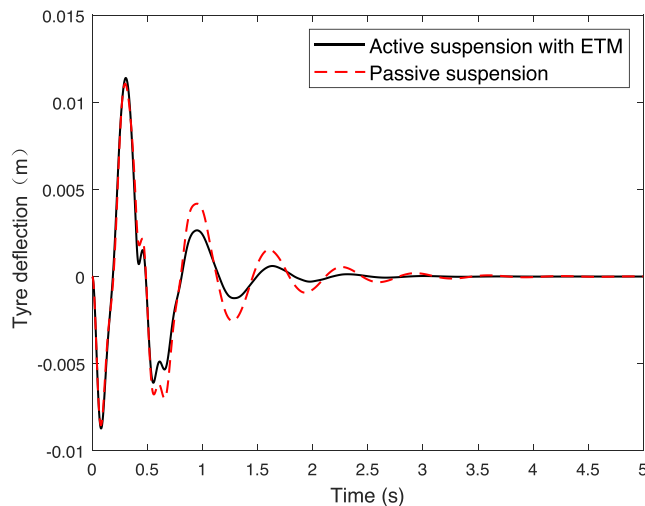


**Fig. 5.** Tyre deflection.

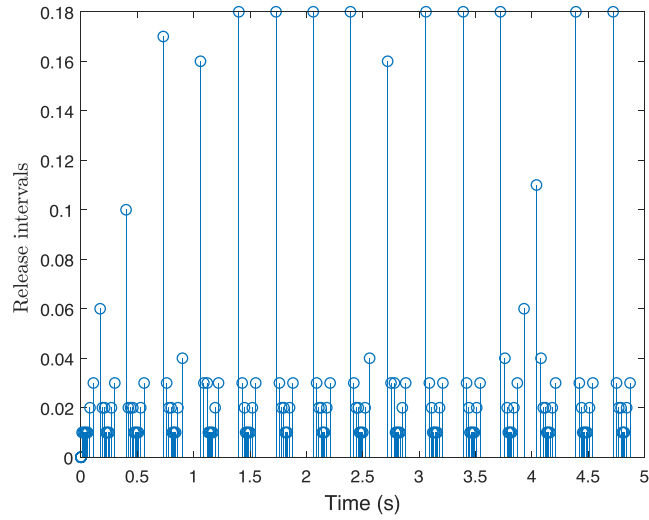


Fig. 6. Release intervals under Case i).

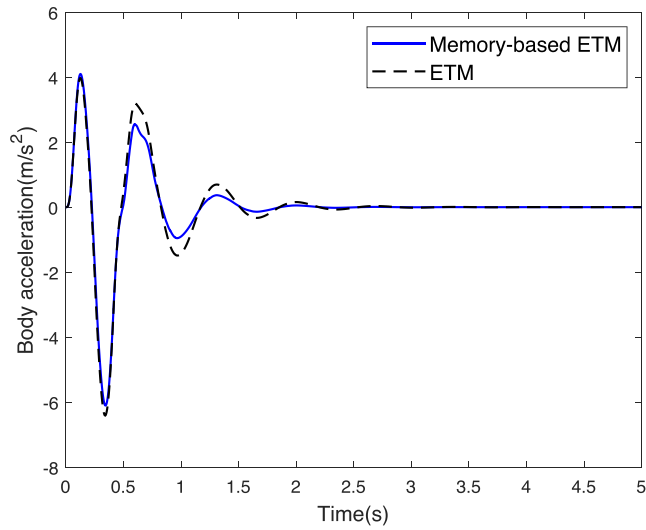


Fig. 7. Body acceleration.

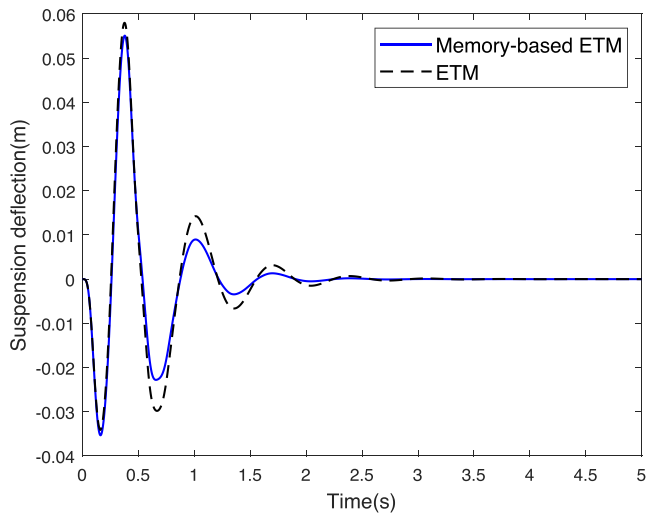


Fig. 8. Suspension deflection.

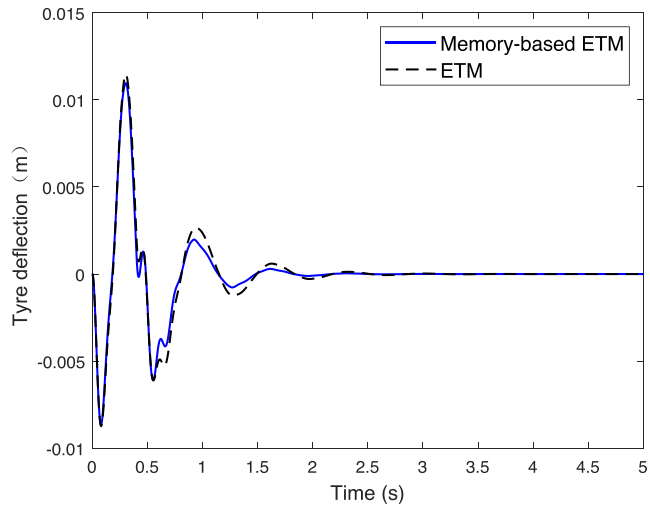


Fig. 9. Tyre deflection.

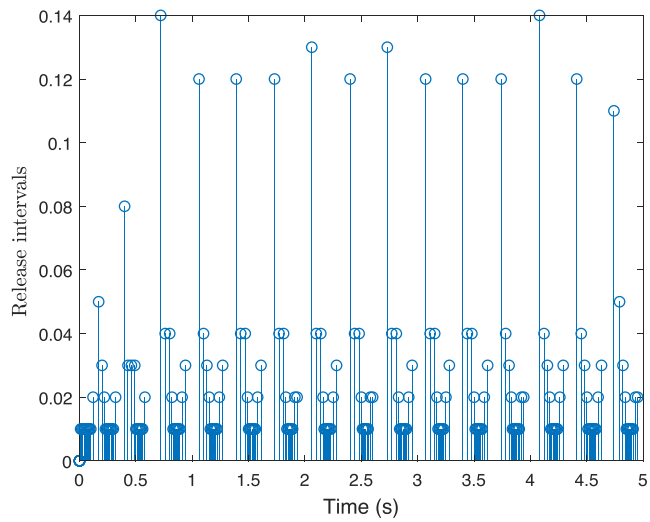


Fig. 10. Release intervals under Case ii).

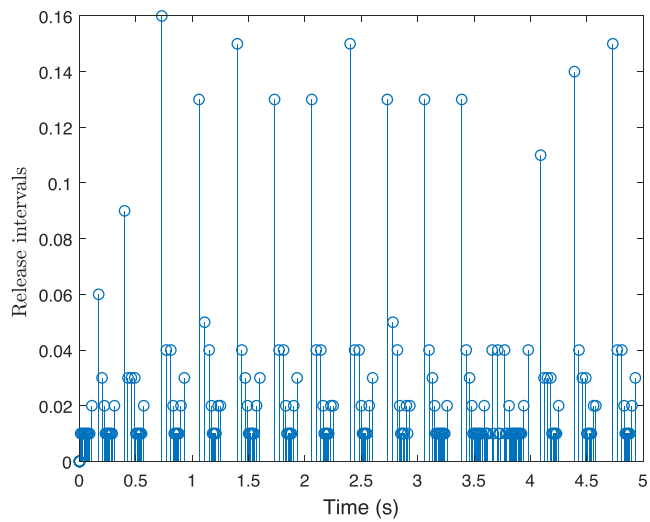


Fig. 11. Release intervals under Case iii).

## 5. Conclusion

In this paper, the problem of  $H_\infty$  memory-based fuzzy controller design has been studied for the cloud-aided ASS against deception attacks. T-S fuzzy model is applied to model the nonlinearity of ASSs caused by the structural features of vehicle and the variation of passengers. To deal with the problem of the limited network bandwidth and insecure wireless networked ASSs, a new memory-based ETM was proposed, by which the average data releasing rate can be greatly decreased, while a satisfied suspension performance under deception attacks was guaranteed by memory-based fuzzy controller. Compared to the traditional ETM, the memory-based ETM we proposed can mitigate the occurrence of false triggering event due to some sudden changes in ETM input, besides, it can increase the releasing rate when the system is subject to external disturbance and deception attacks, which leads to a better control performance of the system. The efficiency of the proposed memory-based ETM has been illustrated by a real quarter-vehicle suspension system. In future work, the problem of secure control by utilizing the memory-based ETM to improve control performance under denial-of-service (DoS) attacks will be an interesting and challenging issue to be investigated. Furthermore, some engineering issues such as state estimation of power systems and sensor networks are worth studying by the methods with memory-based ETM as well.

## Declaration of Competing Interest

The authors declare that they have no known competing financial interests or personal relationships that could have appeared to influence the work reported in this paper.

## Acknowledgement

This work was supported in part by the National Natural Science Foundation of China under Grant 61473156, and in part by the Fundamental Research Funds for the Central Universities, No. 30919011409.

## References

- [1] A.-Y. Lu, G.-H. Yang, Distributed consensus control for multi-agent systems under denial-of-service, *Inf. Sci.* 439 (2018) 95–107.
- [2] D. Ding, Q.-L. Han, Y. Xiang, X. Ge, X.-M. Zhang, A survey on security control and attack detection for industrial cyber-physical systems, *Neurocomputing*. 275 (2018) 1674–1683.
- [3] L. Ding, Q.-L. Han, B. Ning, D. Yue, Distributed resilient finite-time secondary control for heterogeneous battery energy storage systems under denial-of-service attacks, *IEEE Trans. Ind. Inform.* 16 (7) (2020) 4909–4919.
- [4] L. Ding, Q.-L. Han, X.-M. Zhang, Distributed secondary control for active power sharing and frequency regulation in islanded microgrids using an event-triggered communication mechanism, *IEEE Trans. Ind. Inform.* 15 (7) (2019) 3910–3922.
- [5] D. Du, C. Zhang, H. Wang, X. Li, H. Hu, T. Yang, Stability analysis of token-based wireless networked control systems under deception attacks, *Inf. Sci.* 459 (2018) 168–182.
- [6] H. Gao, W. Sun, P. Shi, Robust sampled-data  $H_\infty$  control for vehicle active suspension systems, *IEEE Trans. Contr. Syst. Technol.* 18 (1) (2010) 238–245.
- [7] X. Ge, Q.-L. Han, M. Zhong, X.-M. Zhang, Distributed krein space-based attack detection over sensor networks under deception attacks, *Automatica*. 109 (2019) 108557.
- [8] Z. Gu, S. Fei, Y. Zhao, E. Tian, Robust control of automotive active seat-suspension system subject to actuator saturation, *J. Dyn. Syst. Meas. Contr.* 136 (4) (2014) 041022..
- [9] Z. Gu, P. Shi, D. Yue, Z. Ding, Decentralized adaptive event-triggered  $H_\infty$  filtering for a class of networked nonlinear interconnected systems, *IEEE Trans. on Cybernet.* 49 (5) (2019) 1570–1579.
- [10] H. Li, X. Jing, H.-K. Lam, P. Shi, Fuzzy sampled-data control for uncertain vehicle suspension systems, *IEEE Trans. on Cybernet.* 44 (7) (2014) 1111–1126.
- [11] H. Li, Z. Zhang, H. Yan, X. Xie, Adaptive event-triggered fuzzy control for uncertain active suspension systems, *IEEE Trans. Cybernet.* 49 (12) (2019) 4388–4397.
- [12] J. Liu, T. Yin, J. Cao, D. Yue, H.R. Karimi, Security control for T-S fuzzy systems with adaptive event-triggered mechanism and multiple cyber-attacks, *IEEE Trans. Syst. Man Cybernet. Syst.* (2020), <https://doi.org/10.1109/TSMC.2019.2963143>.
- [13] J. Liu, Y. Gu, L. Zha, Y. Liu, Event-triggered  $H_\infty$  load frequency control for multiarea power systems under hybrid cyber attacks, *IEEE Trans. Syst. Man Cybernet. Syst.* 49 (8) (2019) 1665–1678.
- [14] T. Liu, Z.-P. Jiang, A small-gain approach to robust event-triggered control of nonlinear systems, *IEEE Trans. Autom. Contr.* 60 (8) (2015) 2072–2085.
- [15] Y. Pan, G.-H. Yang, Event-triggered fault detection filter design for nonlinear networked systems, *IEEE Trans. Syst. Man, Cybern. Syst.* 48 (11) (2018) 1851–1862.
- [16] Y. Pan, G.-H. Yang, Novel event-triggered filter design for nonlinear networked control systems, *J. Frankl. Inst.* 355 (3) (2018) 1259–1277.
- [17] P.G. Park, J.W. Ko, C. Jeong, Reciprocally convex approach to stability of systems with time-varying delays, *Automatica*. 47 (1) (2011) 235–238.
- [18] A. Seuret, F. Gouaisbaut, Wirtinger-based integral inequality: Application to time-delay systems, *Automatica*. 49 (9) (2013) 2860–2866.
- [19] E. Tian, C. Peng, Memory-based event-triggering  $H_\infty$  load frequency control for power systems under deception attacks, *IEEE Trans. Cybernet.* (2020), <https://doi.org/10.1109/TCYB.2020.2972384>.
- [20] K. Wang, E. Tian, J. Liu, L. Wei, D. Yue, Resilient control of networked control systems under deception attacks: A memory-event-triggered communication scheme, *Intl. J. Robust Nonl. Contr.* 30 (4) (2020) 1534–1548.
- [21] S. Xiao, Q.-L. Han, X. Ge, Y. Zhang, Secure distributed finite-time filtering for positive systems over sensor networks under deception attacks, *IEEE Trans. Cybernet.* 50 (3) (2020) 1220–1229.
- [22] H. Yan, J. Sun, H. Zhang, X. Zhan, F. Yang, Event-triggered  $H_\infty$  state estimation of 2-dof quarter-car suspension systems with nonhomogeneous markov switching, *IEEE Trans. on Sys. Man Cybernet. Syst.* (2018), <https://doi.org/10.1109/TSMC.2018.2852688>.
- [23] M. Yang, C. Peng, G. Li, Y. Wang, S. Ma, Event-triggered  $H_\infty$  control for active semi-vehicle suspension system with communication constraints, *Inf. Sci.* 486 (2019) 101–113.
- [24] Y. Yang, D. Yue, C. Dou, Output-based event-triggered schemes on leader-following consensus of a class of multi-agent systems with lipschitz-type dynamics, *Inf. Sci.* 459 (2018) 327–340.
- [25] D. Ye, T.-Y. Zhang, Summation detector for false data-injection attack in cyber-physical systems, *IEEE Trans. Cybern.* 50 (6) (2020) 2338–2345.

- [26] D. Ye, N. Diao, X. Zhao, Fault-tolerant controller design for general polynomial-fuzzy-model-based systems IEEE Trans. Fuzzy Syst. 26 (2) (2018) 1046–1051.
- [27] Z. Ye, H. Ni, Z. Xu, D. Zhang, Sensor fault estimation of networked vehicle suspension system with deny-of-service attack, IET Intell. Transp. Syst. 14 (5) (2020) 455–462.
- [28] D. Yue, E. Tian, Q.-L. Han, A delay system method for designing event-triggered controllers of networked control systems, IEEE Trans. Autom. Control. 58 (2) (2013) 475–481.
- [29] B.-L. Zhang, Q.-L. Han, X.-M. Zhang, Event-triggered  $H_{\infty}$  reliable control for offshore structures in network environments, J. Sound Vib. 368 (2016) 1–21.
- [30] D. Zhang, Q.-L. Han, X.-M. Zhang, Network-based modeling and proportional-integral control for direct-drive-wheel systems in wireless network environments, IEEE Trans. Cybern. 50 (6) (2020) 2462–2474.
- [31] H. Zhang, Q. Hong, H. Yan, F. Yang, G. Guo, Event-based distributed  $H_{\infty}$  filtering networks of 2-DoF quarter-car suspension systems, IEEE Trans. Ind. Inf. 13 (1) (2017) 312–321.
- [32] H. Zhang, X. Zheng, H. Yan, C. Peng, Z. Wang, Q. Chen, Co-design of event-triggered and distributed  $H_{\infty}$  filtering for active semi-vehicle suspension systems, IEEE/ASME Trans. Mech. 22 (2) (2017) 1047–1058.
- [33] X.-M. Zhang, Q.-L. Han, Event-triggered  $H_{\infty}$  control for a class of nonlinear networked control systems using novel integral inequalities, Int. J. Robust Nonlin. Control. 27 (4) (2017) 679–700.
- [34] X.-M. Zhang, Q.-L. Han, X. Ge, D. Ding, An overview of recent developments in Lyapunov-Krasovskii functionals and stability criteria for recurrent neural networks with time-varying delays, Neurocomputing. 313 (2018) 392–401.
- [35] X.-M. Zhang, Q.-L. Han, X. Ge, D. Ding, L. Ding, D. Yue, C. Peng, Networked control systems: A survey of trends and techniques, IEEE/CAA J. Autom. Sinica. 7 (1) (2020) 1–17.
- [36] X.-M. Zhang, Q.-L. Han, X. Ge, L. Ding, Resilient control design based on a sampled-data model for a class of networked control systems under denial-of-service attacks, IEEE Trans. Cybern. (2019), <https://doi.org/10.1109/TCYB.2019.2956137>.
- [37] X. Zheng, H. Zhang, H. Yan, F. Yang, L. Vlacic, Active full-vehicle suspension control via cloud-aided adaptive backstepping approach, IEEE Trans. Cybern. (2019), <https://doi.org/10.1109/TCYB.2019.2891960>.